An M-Ary Orthogonal Multilevel Differential Chaos Shift Keying System With Code Index Modulation

Xiangming Cai, Weikai Xu, *Member, IEEE*, Deqing Wang, Shaohua Hong, *Member, IEEE*, and Lin Wang, *Senior Member, IEEE*

***Abstract*— In this paper, an M-ary orthogonal multilevel differential chaos shift keying system with code index modulation (CIM-OM-MDCSK) is proposed. In the proposed system, the multiple information bearing signals are modulated by the selected Walsh codes with specific indices and the M-ary information signals which are composed of modulated bits, chaotic signals, and their Hilbert transform. Since the reference signal along with the information bearing signals are overlapping in time domain and orthogonal in code domain by using Walsh code sequences, the spectral efficiency of the CIM-OM-MDCSK system is improved largely. By combining the M-ary modulation, orthogonal multilevel modulation, and code index modulation, the proposed CIM-OM-MDCSK system can achieve high data rate and superior bit error rate (BER) performance compared to its rivals. Moreover, we derive the BER expressions of the proposed system over additive white Gaussian noise and multipath Rayleigh fading channels. Finally, we make a performance comparison between the proposed system and other state-of-the-art non-coherent chaotic communication systems. The results confirm the competitive benefits of the proposed system.**

***Index Terms*— Chaotic communication, M-ary modulation, multilevel modulation, code index modulation, bit error rate (BER).**

I. Introduction

THE most important challenge for current and future wireless communication is the development of robust communication systems with high data rate. By employing spread-spectrum (SS) techniques, the effect of jamming can be substantially reduced, permitting satisfactory recovery of the information. Chaotic signals, with their inherent wideband characteristic, are natural candidates for spread-spectrum communication [1]–[3] and ultra-wideband communication [4]–[6]. Moreover, chaotic communication systems possess excellent robustness to defense the adverse effect of channel frequency selectivity. Therefore, chaotic communication systems have drawn a great deal of attentions and interests for many research partners.

In 1992, the digital chaotic modulation was first presented by Parlitz *et al.* [7]. Based on this work, the researches on chaotic modulation enter the fast track of development. Since differential chaos shift keying (DCSK) [8] system is equipped with a simple auto-correlation receiver (AcR) and offers excellent performance over multipath fading and time-varying channels [9], DCSK scheme has been extensively researched in various communication scenarios, such as wireless personal area networks (WPANs) [10], multiple input and multiple output (MIMO) systems [11], cooperative communication systems [12], power line communication systems [13], continuous mobility communication systems [14] and simultaneous wireless wireless information and power transfer systems [15]. In conventional DCSK scheme, each bit duration is equally divided into two consecutive time slots. To be specific, the chaotic reference signal is sent in the first time slot, while the data-modulated time-delayed reference signal (referred to as information bearing signal) is arranged in adjacent second time slot. Since half of the bit duration is provided for transmitting non-information-bearing reference samples [1], DCSK scheme will be inevitably restrained by several drawbacks such as inferior data rate, additional energy consumption and the usage of long wideband radio frequency (RF) delay lines, which inspire many research buddies to conduct in-depth researches and explorations on DCSK scheme and other meritorious chaotic communication systems for the purpose of higher data rate and energy efficiency.

Clearly, the popularization of mobile devices has given rise to an exponential increase in data traffic which shows no sign of being abated. Thus, the tremendous demands of high data rate and energy efficiency are, and will continue to be significant elements for wireless communication systems. In this vein, many meritorious chaotic modulation schemes have been reported to improve the data rate and energy efficiency. Starting by the early work of [16], quadrature chaos shift keying (QCSK) system is proposed to achieve double data rate with respect to DCSK system with the same bandwidth occupation, where the chaotic signal and its orthogonal chaotic signal converted by the Hilbert filter can make a linear combination to encode four symbols. With the

Manuscript received November 27, 2018; revised February 28, 2019; accepted March 22, 2019. Date of publication March 29, 2019; date of current version July 13, 2019. This work was supported by the National Natural Science Foundation of China under Grant No. 61671395 and 61871337. The associate editor coordinating the review of this paper and approving it for publication was A. Nallanathan. *(Corresponding author: Deqing Wang.)*

The authors are with the Department of Information and Communication Engineering, Xiamen University, Xiamen 361005, China (e-mail: samson0102@qq.com; xweikai@xmu.edu.cn; deqing@xmu.edu.cn; hongsh@xmu.edu.cn; wanglin@xmu.edu.cn).

Color versions of one or more of the figures in this paper are available online at http://ieeexplore.ieee.org.

Digital Object Identifier 10.1109/TCOMM.2019.2908367

aforementioned motivation, a circle-constellation-based M-ary DCSK system is proposed in [17], which can satisfy higher data rate requirement than QCSK system and provide slightly better BER performance than M-ary PSK-DCSK system (MPSK-DCSK) [18].

Although the DCSK system with M-ary modulation technology can make great strides in the aspect of improving the data rate and energy efficiency, this improvement is at the expense of loss of BER performance. As the modulation order increases which means higher data rate, the Euclidean distance of adjacent constellation points diminishes ineluctably which degrades the BER performance. In order to surmount the weakness of low data rate and energy efficiency, a multilevel DCSK system is presented in [19], which uses the Walsh code sequences to transmit more bits without the penalty of BER performance. Unfortunately, the demand of many RF delay lines at its receiver will create obstacles to its practical application. Then, code-shifted DCSK (CS-DCSK) [20] and its generalized version (GCS-DCSK) [21] are proposed to avoid the usage of delay lines at the receiver. Enjoying the excellent orthogonality of different chaotic sequences, an extension of CS-DCSK system called high-data-rate CS-DCSK (HCS-DCSK) [22] can offer high data rate and strengthen data security, where its reference and information bearing signals are separated by different chaotic sequences rather than finite Walsh code sequences.

To further improve the data rate and BER performance of CS-DCSK system, a novel multilevel CS-DCSK (MCS-DCSK) system is presented in [23], where its performance is improved with the increasing of the number of data streams. The latest multilevel modulation scheme referred to as orthogonal multilevel DCSK (OM-DCSK) is reported in [24]. In this configuration, its information bearing signals are chosen from the orthogonal signal set established by original reference signal. In the view of data rate, more information bearing signals mean higher data rate. Thus, the authors combine the chaotic signals and their Hilbert transforms with Walsh codes to augment the number of information bearing signals within the orthogonal signal set. In summary, all of the above multilevel modulation schemes possess a same characteristic that the reference signal and information bearing signal are overlapping in time domain, thus higher data rate and spectral efficiency turn attainable.

There has been a growing interest on index modulation (IM) techniques over the past few years. IM techniques, which are considered innovative ways to convey information compared to traditional communication systems, appear as competitive candidates for next generation wireless networks due to the attractive advantages they offered in terms of spectral and energy efficiency as well as hardware simplicity [25]. In this vein, a novel non-coherent chaotic modulation system named commutation code index DCSK (CCI-DCSK) is presented in [26], where the additional mapped bits are carried by various commutated replicas of reference chaotic sequence. Moreover, since the reference signal and orthogonal data bearing signal are summed within the same time slot, the data rate and spectral efficiency of CCI-DCSK augments in an outstanding manner. Permutation index DCSK (PI-DCSK) [27] is proposed with the target of heightening the data rate and energy efficiency. In PI-DCSK system, after establishing diverse quasi-orthogonal sequence sets which are formed by permuting the reference sequence, extra bits are transmitted by means of the specific indices of the quasi-orthogonal sequences.

Another promising and competitive modulation technique called code index modulation (CIM) [28], [29] has been developed aiming to enhance data rate and reduce energy consumption while being simple to implement. Actually, it has been proven that in comparison with spatial modulation (SM), CIM technique has better energy efficiency, higher spectral efficiency and requires less multiplication operations while being simple to implement in terms of hardware [30]. Benefiting from CIM and multilevel modulation, the multilevel chaotic modulation scheme with code index modulation, namely CIM-CS-DCSK [31], can obtain higher data rate than GCS-DCSK scheme, where additional information bits are carried by specific indices of Walsh codes. More recently, a novel short reference DCSK (SR-DCSK) [32] with code index modulation referred to as CIM-DCSK is reported in [33]. Besides, to further improve the BER performance of CIM-DCSK system, two additional optimization techniques have also been elaborated: the noise-reduction method [34] and the power-coefficient optimization algorithm [35].

A. Motivations and Contributions

Since the chaotic signals were born, they have triggered rapid advances in the field of chaotic communication, especially for the case of non-coherent chaotic modulation communication systems. Numerous research buddies have made a large amount of efforts devoted to researching high-data-rate and high-performance non-coherent chaotic modulation schemes. Motivated by the works of [17], [24], [29] and [34], the M-ary modulation, multilevel modulation, code index modulation and DCSK can make a powerful combination to achieve high data rate, high spectral efficiency and excellent performance. Accordingly, we propose an M-ary orthogonal multilevel differential chaos shift keying system with code index modulation, namely CIM-OM-MDCSK, which shows preeminent and competitive BER performance with high data rate and spectral efficiency. The main contributions of this paper are summarized as follows:

- An M-ary orthogonal multilevel differential chaos shift keying system with code index modulation is proposed and analyzed in an exhaustive manner.
- Enjoying the M-ary modulation, multilevel modulation and code index modulation, the proposed CIM-OM-MDCSK system can achieve higher data rate, higher spectral efficiency and better BER performance than other non-coherent chaotic communication systems.
- The analytical BER expressions of the proposed system over AWGN and multipath Rayleigh fading channels are analyzed and derived in an elaborative manner, then we simulate the proposed system and the simulation results confirm our derivations.

The remainder of this paper is organized as follows. The next section presents the CIM-OM-MDCSK system. Performance analysis of the proposed system is provided in

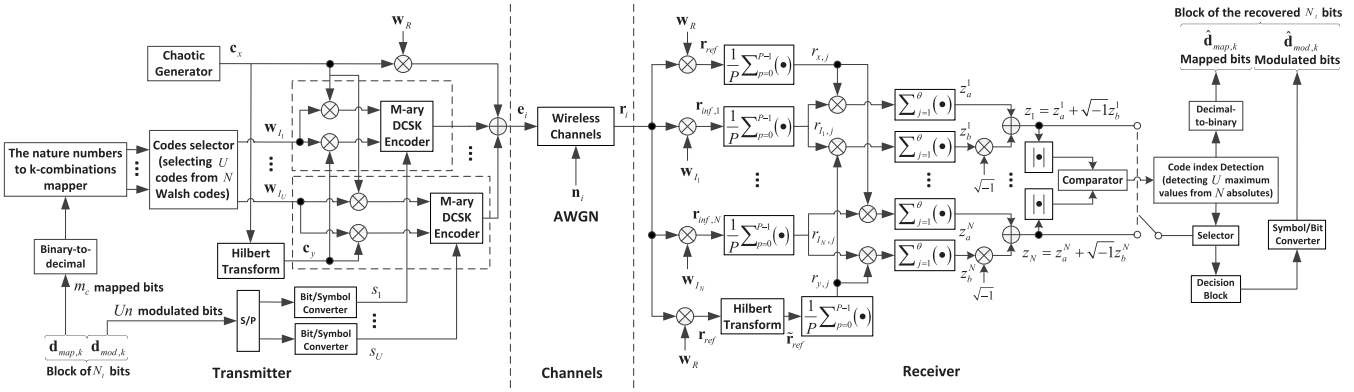

Fig. 1. The block diagram of CIM-OM-MDCSK system.

Section III. In Section IV, the numerical results and discussions are given. Section V concludes this paper.

II. CIM-OM-MDCSK System

A. The Transmitter

The block diagram of the proposed CIM-OM-MDCSK system is shown in Fig. 1. In general, the total transmitted bits are split into several blocks with N_t bits per block. The first subblock with length m_c bits is termed as mapped bits, and then the second subblock with length Un bits is referred to as the modulated bits which is provided for physically transmission, where n is the number of modulated bits per M-ary DCSK encoder, U is the number of information bearing signals per transmitted symbol. Accordingly, the total number of transmitted bits per block is $N_t = m_c + Un$ and the k^{th} block of transmitted bits can be expressed in vector form as $\mathbf{d}_k = [d_{1,k}, d_{2,k}, \cdots, d_{m_c+Un,k}] = [\mathbf{d}_{map,k}, \mathbf{d}_{mod,k}]$, where $\mathbf{d}_{map,k}$ and $\mathbf{d}_{mod,k}$ denote the vector of mapped bits and modulated bits, respectively.

At the transmitter, the overall transmitted signal within a symbol duration is the sum of the reference signal and numerous information bearing signals. If the single isolated symbol during transmission is considered, the baseband discrete transmitted signal of the i^{th} CIM-OM-MDCSK symbol $\mathbf{e}_i$ can be represented as

$$\mathbf{e}_i = \mathbf{w}_R \otimes \mathbf{c}_x + \sum_{u=1}^{U} \mathbf{w}_{I_u} \otimes (a_u \mathbf{c}_x + b_u \mathbf{c}_y), \tag{1}$$

where $\mathbf{c}_x = [c_{x,1}, c_{x,2}, \cdots, c_{x,\theta}]$ is a θ-length chaotic sequence and $\mathbf{c}_y$ is its orthogonal chaotic sequence, which is constructed by Hilbert transform. $\otimes$ is kronecker product operator. $\mathbf{w}_R = [w_{R,1}, w_{R,2}, \cdots, w_{R,P}]$ denotes a Walsh code sequence with length P used to carry the reference signal. Without loss of generality, we assume the last row of Walsh code matrix is arranged for reference signal. Then, $\mathbf{w}_{I_u} = [w_{I_u,1}, w_{I_u,2}, \cdots, w_{I_u,P}], u = 1, 2, \cdots U$ are several Walsh codes with code indices $\{I_u\}_{u=1}^{U}$ provided for information bearing signals, where the specific indices are chosen from a code set $\{\mathbf{w}_{I_u}\}_{u=1}^{N}$ including N Walsh codes, where $N = P - 1$. Particularly, the selected code indices $\{I_u\}_{u=1}^{U}$ are obtained by the natural numbers to k-combinations mapping method introduced in [31]. Therefore, the number of mapped bits can be calculated as $m_c = \left\lfloor \log_2 \left[\binom{N}{U} \right] \right\rfloor$, where $\binom{N}{U} = \frac{N!}{U!(N-U)!}$ denotes combination number and $\lfloor \bullet \rfloor$ is floor function. We define the spreading factor of the CIM-OM-MDCSK system as $\beta = P\theta$. In addition, a_u and b_u are real part and imaginary part of the M-ary constellation symbol s_u corresponding to the u^{th} information symbol (see a case of 16-ary DCSK in Fig. 2). The M-ary constellation symbol s_u can be expressed as

$$s_u = \cos\left(2\pi \frac{m-1}{M} + \phi_u\right) + \sqrt{-1} \sin\left(2\pi \frac{m-1}{M} + \phi_u\right), \quad m = 1, 2, \cdots, M, \tag{2}$$

where ϕ_u means the initial phase angle of the u^{th} M-ary constellation symbol. Besides, $M = 2^n$ denotes the modulation order of M-ary DCSK.

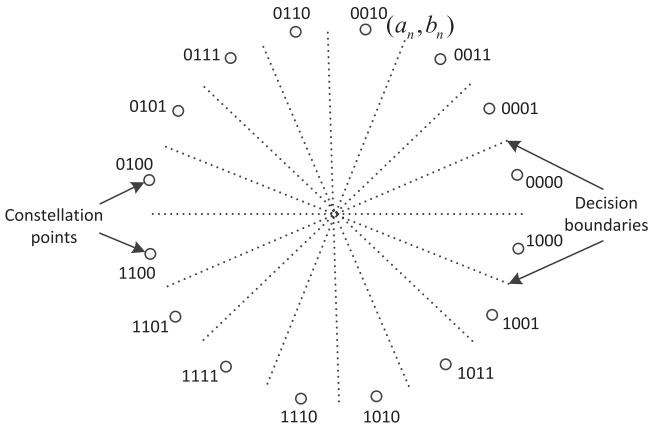

Fig. 2. 16-ary DCSK constellation with Gray code mapping and its decision boundaries.

B. The Receiver

Assuming that the transmitted signal is corrupted by multipath fading and additive white Gaussian noise, the received baseband discrete signal can be stated as

$$\mathbf{r}_i = \sum_{l=1}^{L} \alpha_{i,l} \mathbf{e}_{i,\tau_{i,l}} + \mathbf{n}_i, \tag{3}$$

where L is the number of path, $\alpha_{i,l}$ and $\tau_{i,l}$ are the channel coefficient and the path delay of the l^{th} path, respectively.

Then, $\mathbf{n}_i$ denotes the additive white Gaussian noise vector with zero mean and covariance $\frac{N_0}{2}\mathbf{I}$, where $\mathbf{I}$ is an identity matrix. Note that when the channel parameters satisfy $L = 1$, a unit channel coefficient $\alpha_{i,1} = 1$ and zero time delay $\tau_{i,1} = 0$, the channel degrades into the case of AWGN channel. In this paper, a classical slow fading channel model [36]–[38] with Rayleigh distributed channel coefficients is adopted. The Rayleigh probability density function (PDF) of the channel coefficients is given by

$$f_\alpha(z) = \frac{z}{\ell^2}\exp\left(-\frac{z^2}{2\ell^2}\right), \tag{4}$$

where $\ell > 0$ is the scale parameter of the distribution.

The receiver structure of the proposed CIM-OM-MDCSK system is depicted in Fig. 1. Clearly, the received baseband discrete signal can be represented in a vector form as $\mathbf{r}_i = [r_{1,i}, r_{2,i}, \cdots, r_{P\theta,i}]$ and the subscript i will be omitted in the following analysis for simplification. Firstly, we extract the reference signal and different information bearing signals from the received signal by using different Walsh codes described as

$$\mathbf{r}_{ref} = \mathbf{r} \odot (\mathbf{w}_R \otimes \mathbf{1}_{1\times\theta}), \tag{5}$$

$$\mathbf{r}_{inf,u} = \mathbf{r} \odot (\mathbf{w}_{I_u} \otimes \mathbf{1}_{1\times\theta}), \quad u = 1, 2, \cdots, N, \tag{6}$$

where $\mathbf{1}_{1\times\theta}$ is an identity vector with a row and θ columns, $\odot$ is Hadamard product operator. Besides, $\tilde{\mathbf{r}}_{ref} = \mathcal{H}(\mathbf{r}_{ref})$ is the Hilbert transform of $\mathbf{r}_{ref}$, where $\mathcal{H}(\bullet)$ denotes Hilbert transform operation. Then, the signals $\mathbf{r}_{ref}$, $\tilde{\mathbf{r}}_{ref}$ and $\mathbf{r}_{inf,u}$ are averaged with a size of P. Therefore, the recovered reference signals $r_{x,j}$ for in-phase component can be represented as (7), as shown at the bottom of this page. The term shown in the second line of (7) equals zero, which is due to the fact that $w_{R,p+1}$ and $w_{I_u,p+1}$ denote the different Walsh code sequences and they are orthogonal to each other.

Similarly, the recovered reference signals $r_{y,j}$ for quadrature component and the recovered information bearing signals $r_{I_u,j}$ can be obtained as

$$r_{y,j} = \sum_{l=1}^{L} \alpha_l c_{y,j-\tau_l} + \tilde{n}_{R,j}, \tag{8}$$

$$r_{I_u,j} = \sum_{l=1}^{L} \alpha_l \left(a_u c_{x,j-\tau_l} + b_u c_{y,j-\tau_l}\right) + n_{I_u,j}, \quad u = 1, 2, \cdots, N, \tag{9}$$

where $0 < j \le \theta$. Besides, $n_{R,j}$, $\tilde{n}_{R,j}$ and $n_{I_u,j}$ are AWGN with zero mean and variance $\frac{N_0}{2P}$ [34], where $\tilde{n}_{R,j} = \mathcal{H}(n_{R,j})$. Subsequently, the decision variables of in-phase branch and quadrature branch corresponding to the correlator of the u^{th} symbol are given as $z_a^u = \sum_{j=1}^{\theta} r_{x,j} r_{I_u,j}$ and $z_b^u = \sum_{j=1}^{\theta} r_{y,j} r_{I_u,j}$, respectively. The linear combination of the decision variables z_a^u and z_b^u is stated as $z_u = z_a^u + \sqrt{-1} z_b^u$. Particularly, let $|\mathbf{z}| = \{|z_1|, |z_2|, \cdots, |z_N|\}$, thus we can estimate U indices $\left\{\hat{I}_u\right\}_{u=1}^{U}$ by selecting U maximums from the set $|\mathbf{z}|$ via the code indices estimation algorithm [31]. Then, we use set $|\mathbf{z}'|$ to represent the selected U maximums, namely $|\mathbf{z}'| = \{|z_1'|, |z_2'|, \cdots, |z_U'|\}$. Hence, the M-ary constellation symbols corresponding to the above U indices can be estimated by the minimum distance decision criterion described as

$$\hat{s}_u = \arg\min_{s\in S} \left(|z_u' - s|^2\right), \quad u = 1, 2, \cdots, U, \tag{10}$$

where S denotes the M-ary constellation point sets. Finally, the mapped bits can be recovered by converting the selected indices from the decimal number to binary number, while the modulated bits can be recovered by the symbol-to-bit converter.

C. Hardware Complexity and Spectral Efficiency Comparison

In this subsection, the hardware complexity and spectral efficiency of the proposed CIM-OM-MDCSK system are compared with the counterparts of other chaotic communication systems. We start analyzing the hardware complexity of CIM-OM-MDCSK system. Table I and Table II exhibit the elements used to constitute CIM-OM-MDCSK, PI-DCSK and CIM-DCSK transmitters and receivers, respectively. In order to realize the M-ary modulation, the Hilbert filter is prerequisite for the proposed CIM-OM-MDCSK system in both transmitter and receiver. In addition, the implement of k-combinations mapper and several delay units make CIM-OM-MDCSK system more complicated in contrast to PI-DCSK and CIM-DCSK systems. However, it is by means of the price of hardware complexity that the proposed CIM-OM-MDCSK system harvests the improvement of the data rate and BER performance to a great extent. In other words, there is a trade-off in terms of hardware complexity, data rate and BER performance in the proposed CIM-OM-MDCSK system.

The spectral efficiency comparison between CIM-OM-MDCSK system and other non-coherent IM-based chaotic

$$\begin{aligned} r_{x,j} &= \frac{1}{P}\sum_{p=0}^{P-1} w_{R,p+1}\left[\sum_{l=1}^{L}\alpha_l\left(w_{R,p+1}c_{x,p\theta+j-\tau_l} + w_{I_u,p+1}\left(a_u c_{x,p\theta+j-\tau_l} + b_u c_{y,p\theta+j-\tau_l}\right)\right) + n_{p\theta+j}\right] \\ &= \frac{1}{P}\sum_{p=0}^{P-1}\sum_{l=1}^{L}\alpha_l w_{R,p+1}^2 c_{x,p\theta+j-\tau_l} + \underbrace{\frac{1}{P}\sum_{p=0}^{P-1}\sum_{l=1}^{L}\alpha_l w_{R,p+1} w_{I_u,p+1}\left(a_u c_{x,p\theta+j-\tau_l} + b_u c_{y,p\theta+j-\tau_l}\right)}_{=0} + \frac{1}{P}\sum_{p=0}^{P-1} w_{R,p+1} n_{p\theta+j} \\ &= \sum_{l=1}^{L}\alpha_l c_{x,j-\tau_l} + n_{R,j}. \end{aligned} \tag{7}$$

TABLE I
TRANSMITTER HARDWARE COMPLEXITY COMPARISON

System	CIM-OM-MDCSK	PI-DCSK	CIM-DCSK
Adders	1	0	0
Multipliers	$2U+1$	1	2
Delay units	P	0	P
Selector	Code selector	Permutation selector	Code selector
Modulator	M-ary DCSK modulator	DCSK modulator	DCSK modulator
Other blocks	Hilbert filter, k-combinations mapper, Walsh code generator	Permutation block, Switch	Walsh code generator, Switch

TABLE II
RECEIVER HARDWARE COMPLEXITY COMPARISON

System	CIM-OM-MDCSK	PI-DCSK	CIM-DCSK
Adders	$4P-2$	$\frac{M_t}{2}$ [1]	$2P$
Multipliers	$5P-1$	$\frac{M_t}{2}$	P
Demodulator	M-ary DCSK demodulator	DCSK demodulator	DCSK demodulator
Detection	Code index detection	Index detection	Code index detection
Other blocks	Hilbert filter, Switch, Walsh code generator	Permutation block, Control unit	Walsh code generator, Switch

[1] M_t denotes the special modulation order in PI-DCSK system [27].

TABLE III
SPECTRAL EFFICIENCY COMPARISON

System	Spectral efficiency
CIM-OM-MDCSK	$\frac{m_c+Un}{P\theta B}$
PI-DCSK	$\frac{m_c+1}{2\theta B}$
CIM-DCSK	$\frac{m_c+1}{(P+1)\theta B}$
CSK	$\frac{1}{\theta B}$

communication systems is tabulated in Table III and, additionally, the spectral efficiency of coherent scheme, such as a classical chaos shift keying (CSK) [1], is listed as well for a reference. Assuming that the bandwidth is equal to B in all systems above, the spectral efficiency of CIM-OM-MDCSK system can be formulated as $SE_1 = \frac{m_c+Un}{P\theta B}$. Besides, the spectral efficiency of PI-DCSK, CIM-DCSK and CSK systems can be obtained in a similar manner, described as $SE_2 = \frac{m_c+1}{2\theta B}$, $SE_3 = \frac{m_c+1}{(P+1)\theta B}$ and $SE_4 = \frac{1}{\theta B}$, respectively. Generally, when appropriate system parameters are adopted, the CIM-OM-MDCSK system wins the preferable spectral efficiency compared to its rivals. For example, the increase of modulation order for CIM-OM-MDCSK system can elevate the number of modulated bits per symbol to the benefit of spectral efficiency improvement.

III. PERFORMANCE ANALYSIS

A. BER Analysis of CIM-OM-MDCSK

There are $m_c + Un$ bits transmitted by single CIM-OM-MDCSK symbol, where m_c bits are assigned for the mapped bits and the rest Un bits are arranged for modulated bits, respectively. Therefore, the bit error rate of CIM-OM-MDCSK system is composed of the BER of the mapped bits (P_{map}) and the BER of the modulated bits (P_{mod}). Accordingly, the total bit error rate of CIM-OM-MDCSK system would be stated as

$$P_{sys} = \frac{m_c}{m_c+Un}P_{map} + \frac{Un}{m_c+Un}P_{mod}. \tag{11}$$

When the code indices are erroneously detected, we will obtain a wrong combination of mapped bits. Compared to correct combination, each wrong combination may involve a various number of incorrect mapped bits. Thus, the bit error probability of the mapped bits is a function of error probability of code index detection given as [27]

$$P_{map} = \frac{2^{(m_c-1)}}{2^{m_c}-1}P_{ed}, \tag{12}$$

where P_{ed} denotes erroneous code detection probability. With respect to the BER of the modulated bits, the errors may result from two different cases. In the first case, the code indices are correctly detected, but the modulated bits are recovered with an error. In the second case, code index detection is wrong which results in the error for modulated bits. As a result, the BER of the modulated bits is represented as [29]

$$P_{mod} = P_e\left(1-P_{ed}\right) + \frac{1}{2}P_{ed}, \tag{13}$$

where P_e is the bit error probability of M-ary orthogonal multilevel DCSK. Since the modulated bits still have 50% chance of being correct on the condition of incorrect code index detection, the factor $\frac{1}{2}$ is the error probability of modulated bits when the code index detection is incorrect. Note that

the bit error rate of the CIM-OM-MDCSK system is calculable as long as the BER of M-ary orthogonal multilevel DCSK P_e and the erroneous code detection probability P_{ed} are obtained. Therefore, the error probability P_e and P_{ed} will be analyzed in the following two subsections.

B. BER of M-Ary Orthogonal Multilevel DCSK P_e

Since all the information bearing signals corresponding to the selected code indices are independent and have the same error probability, we only need to evaluate the error performance of one of them. According to the block diagram of the proposed CIM-OM-MDCSK system, the decision variable of u^{th} in-phase branch is given as

$$\begin{aligned} z_a^u &= \sum_{j=1}^{\theta}\left(\sum_{l=1}^{L}\alpha_l c_{x,j-\tau_l}+n_{R,j}\right) \\ &\quad\times\left(\sum_{l=1}^{L}\alpha_l\left(a_u c_{x,j-\tau_l}+b_u c_{y,j-\tau_l}\right)+n_{I_u,j}\right) \\ &= \sum_{j=1}^{\theta}\sum_{l=1}^{L}\alpha_l^2 a_u c_{x,j-\tau_l}^2+\underbrace{\sum_{j=1}^{\theta}\sum_{l=1}^{L}\alpha_l^2 b_u c_{x,j-\tau_l}c_{y,j-\tau_l}}_{=0} \\ &\quad+\sum_{j=1}^{\theta}\sum_{l=1}^{L}\alpha_l\left(a_u c_{x,j-\tau_l}+b_u c_{y,j-\tau_l}\right)n_{R,j} \\ &\quad+\sum_{j=1}^{\theta}\sum_{l=1}^{L}\alpha_l c_{x,j-\tau_l}n_{I_u,j}+\sum_{j=1}^{\theta}n_{R,j}n_{I_u,j}. \end{aligned} \tag{14}$$

Therefore, the mean and variance of the decision variable z_a^u can be calculated as

$$\mathrm{E}\left[z_a^u\right]=\sum_{l=1}^{L}\alpha_l^2 a_u\theta\mathrm{E}\left[c_j^2\right]=\sum_{l=1}^{L}\alpha_l^2\frac{a_u E_s}{P\left(1+U\right)}, \tag{15}$$

$$\begin{aligned} \mathrm{Var}\left[z_a^u\right] &= \sum_{l=1}^{L}\alpha_l^2\left(1+a_u^2+b_u^2\right)\theta\mathrm{E}\left[c_j^2\right]\frac{N_0}{2P}+\theta\frac{N_0^2}{4P^2} \\ &= \sum_{l=1}^{L}\alpha_l^2\frac{E_s N_0}{P^2\left(1+U\right)}+\theta\frac{N_0^2}{4P^2}, \end{aligned} \tag{16}$$

where $\mathrm{E}\left[\bullet\right]$ and $\mathrm{Var}\left[\bullet\right]$ are the expectation operator and variance operator, respectively. In addition, E_s denotes the symbol energy of CIM-OM-MDCSK which satisfies $E_s = P\theta\left(1+U\right)\mathrm{E}\left[c_j^2\right]$, where $\mathrm{E}\left[c_j^2\right]=\mathrm{E}\left[c_{x,j-\tau_l}^2\right]=\mathrm{E}\left[c_{y,j-\tau_l}^2\right]$. Since the decision variable z_a^u and z_b^u are symmetric, the mean and variance of z_b^u are given in a similar manner as

$$\mathrm{E}\left[z_b^u\right]=\sum_{l=1}^{L}\alpha_l^2\frac{b_u E_s}{P\left(1+U\right)}, \tag{17}$$

$$\mathrm{Var}\left[z_b^u\right]=\sum_{l=1}^{L}\alpha_l^2\frac{E_s N_0}{P^2\left(1+U\right)}+\theta\frac{N_0^2}{4P^2}. \tag{18}$$

It is not difficult to find that the decision variable z_a^u and z_b^u are independent Gaussian variables with means $m_1 = a_u E_m$ and $m_2 = b_u E_m$, respectively, where $E_m = \sum_{l=1}^{L}\alpha_l^2\frac{E_s}{P(1+U)}$. Moreover, both decision variables have the identical variance $\sigma^2 = \sum_{l=1}^{L}\alpha_l^2\frac{E_s N_0}{P^2(1+U)}+\theta\frac{N_0^2}{4P^2}$. As a consequence, the joint probability density function of the decision variables z_a^u and z_b^u is given as

$$p\left(z_a^u, z_b^u\right)=\frac{1}{2\pi\sigma^2}\exp\left(-\frac{\left(z_a^u-m_1\right)^2+\left(z_b^u-m_2\right)^2}{2\sigma^2}\right). \tag{19}$$

In the case of M-ary circular constellation, we usually detect the symbol information by its phase angle. Inspired by this idea, we convert the Cartesian coordinate system to the corresponding polar coordinate system shown as

$$\begin{cases} R=\sqrt{\left(Z_a^u\right)^2+\left(Z_b^u\right)^2}, \\ \Omega=\operatorname{actan}\left(\frac{Z_b^u}{Z_a^u}\right). \end{cases} \tag{20}$$

When (19) is expressed in the form of polar coordinates, it can be rewritten as

$$\begin{aligned} &p_{R,\Omega}(r,\omega) \\ &=\frac{r}{2\pi\sigma^2}\exp\left(-\frac{r^2-2r\left(m_1\cos\omega+m_2\sin\omega\right)+m_1^2+m_2^2}{2\sigma^2}\right). \end{aligned} \tag{21}$$

According to Fig. 2, it is clearly observed that $a_u=\cos\varphi$ and $b_u=\sin\varphi$, where φ denotes the phase angle of the u^{th} constellation point. Taking into consideration $m_1 = a_u E_m$ and $m_2 = b_u E_m$, (21) can be further simplified as

$$\begin{aligned} &p_{R,\Omega}(r,\omega) \\ &=\frac{r}{2\pi\sigma^2}\exp\left(-\frac{r^2-2rE_m\left(\cos\varphi\cos\omega+\sin\varphi\sin\omega\right)+E_m^2}{2\sigma^2}\right) \\ &=\frac{r}{2\pi\sigma^2}\exp\left(-\frac{r^2-2rE_m\cos\psi+E_m^2}{2\sigma^2}\right), \end{aligned} \tag{22}$$

where $\cos\psi=\cos\varphi\cos\omega+\sin\varphi\sin\omega$. Thus, $\psi=\varphi-\omega$, where ψ denotes the phase error between the transmitted signal and the contaminated received signal. In order to get the marginal probability density function of the phase error variable ψ, we integrate the variable r described as

$$p(\psi)=\int_0^{+\infty}\frac{r}{2\pi\sigma^2}\exp\left(-\frac{r^2-2rE_m\cos\psi+E_m^2}{2\sigma^2}\right)\mathrm{d}r. \tag{23}$$

Let $\rho=\frac{E_m}{\sigma}$, $\xi=\frac{r}{\sigma}$ and $\mathrm{d}r=\sigma\mathrm{d}\xi$, the above expression can be rewritten as

$$p(\psi)=\int_0^{+\infty}\frac{\xi}{2\pi}\exp\left(-\frac{\xi^2-2\xi\rho\cos\psi+\rho^2}{2}\right)\mathrm{d}\xi. \tag{24}$$

Then, substituting $\rho^2=\left(\rho\sin\psi\right)^2+\left(\rho\cos\psi\right)^2$ into (24), it clearly shows

$$\begin{aligned} p(\psi) &= \int_0^{+\infty}\frac{\xi}{2\pi}\exp\left(-\frac{\xi^2-2\xi\rho\cos\psi+\rho^2}{2}\right)\mathrm{d}\xi \\ &= \exp\left(-\frac{\left(\rho\sin\psi\right)^2}{2}\right) \\ &\quad\times\underbrace{\int_0^{+\infty}\frac{\xi}{2\pi}\exp\left(-\frac{\left(\xi-\rho\cos\psi\right)^2}{2}\right)\mathrm{d}\xi}_{\chi}, \end{aligned} \tag{25}$$

where the above integral χ can be further simplified as

$$\begin{aligned}\chi &= \int_0^{+\infty} \frac{\xi-\rho\cos\psi}{2\pi}\exp\left(-\frac{(\xi-\rho\cos\psi)^2}{2}\right)\mathrm{d}\xi \\ &\quad + \int_0^{+\infty} \frac{\rho\cos\psi}{2\pi}\exp\left(-\frac{(\xi-\rho\cos\psi)^2}{2}\right)\mathrm{d}\xi \\ &= \frac{1}{2\pi}\exp\left(-\frac{(\rho\cos\psi)^2}{2}\right)+\frac{\rho\cos\psi}{\sqrt{2\pi}}Q\left(-\rho\cos\psi\right). \quad (26)\end{aligned}$$

Therefore, by replacing (26) into (25), $p(\psi)$ can be rewritten as

$$p(\psi)=\frac{\exp\left(-\frac{\rho^2}{2}\right)}{2\pi}+\exp\left(-\frac{\rho^2\sin^2\psi}{2}\right)\frac{\rho\cos\psi}{\sqrt{2\pi}}Q\left(-\rho\cos\psi\right) \quad (27)$$

where $Q(x) = \frac{1}{\sqrt{2\pi}}\int_x^{+\infty}\exp\left(-\frac{t^2}{2}\right)\mathrm{d}t$, $x \geq 0$. Besides, $\rho = \frac{E_m}{\sigma}$, where $E_m = \sum_{l=1}^{L}\alpha_l^2\frac{E_s}{P(1+U)}$ and $\sigma^2 = \sum_{l=1}^{L}\alpha_l^2\frac{E_sN_0}{P^2(1+U)}+\theta\frac{N_0^2}{4P^2}$. As a result, $\rho = \frac{2\gamma_s}{\sqrt{4(1+U)\gamma_s+(1+U)^2\theta}}$, where γ_s is the symbol-SNR defined as $\gamma_s = \sum_{l=1}^{L}\alpha_l^2\frac{E_s}{N_0}$. When the signal-to-noise ratio (SNR) is large and $|\psi| \leq \frac{\pi}{2}$, the term $\frac{\exp\left(-\frac{\rho^2}{2}\right)}{2\pi}$ is approximately equal to zero, while $Q\left(-\rho\cos\psi\right)$ is approximately equal to one. Thus, $p(\psi)$ can be better approximated as

$$p(\psi) \approx \frac{\rho\cos\psi}{\sqrt{2\pi}}\exp\left(-\frac{\rho^2\sin^2\psi}{2}\right). \quad (28)$$

Then, an error appears in phase detection when the phase falls outside the region $\left[-\frac{\pi}{M},\frac{\pi}{M}\right]$. Therefore, the bit error probability can be represented as [38]

$$P_e \approx \frac{1}{n}\left[1-\int_{-\frac{\pi}{M}}^{\frac{\pi}{M}}p(\psi)\mathrm{d}\psi\right]. \quad (29)$$

Finally, substituting (28) into (29), the bit error rate of the M-ary orthogonal multilevel DCSK can be stated as

$$P_e \approx \frac{1}{n}\left[1-\int_{-\frac{\pi}{M}}^{\frac{\pi}{M}}\frac{\rho\cos\psi}{\sqrt{2\pi}}\exp\left(-\frac{\rho^2\sin^2\psi}{2}\right)\mathrm{d}\psi\right]. \quad (30)$$

Substituting $\nu = \rho\sin\psi$ and $\mathrm{d}\nu = \rho\cos\psi\mathrm{d}\psi$ into (30), thus (30) can be rewritten as

$$\begin{aligned}P_e &\approx \frac{1}{n}\frac{2}{\sqrt{2\pi}}\int_{\rho\sin\frac{\pi}{M}}^{+\infty}\exp\left(-\frac{\nu^2}{2}\right)\mathrm{d}\nu \\ &= \frac{2}{n}Q\left(\rho\sin\frac{\pi}{M}\right). \quad (31)\end{aligned}$$

When the modulation order is greater than or equal to 4, i.e., $M \geq 4$, it apparently appears $\sin\frac{\pi}{M} \approx \frac{\pi}{M}$ by means of Taylor approximation. In this vein, the bit error rate of the M-ary orthogonal multilevel DCSK can be expressed in a rather simple form as

$$P_e \approx \frac{2}{n}Q\left(\frac{\rho\pi}{M}\right). \quad (32)$$

In particular, on the condition of $M = 2$, the mean and variance of the M-ary orthogonal multilevel DCSK can be calculated as

$$\mu_s = \sum_{l=1}^{L}\alpha_l^2\frac{E_s}{P(1+U)}, \quad (33)$$

$$\sigma_s^2 = \sum_{l=1}^{L}\alpha_l^2\frac{E_sN_0}{P^2(1+U)}+\theta\frac{N_0^2}{4P^2}. \quad (34)$$

Thus, in this case, Gaussian approximation is applied to obtain the bit error probability of M-ary orthogonal multilevel DCSK shown as

$$\begin{aligned}P_e &= \frac{1}{2}\mathrm{erfc}\left[\left(\frac{2\sigma_s^2}{\mu_s^2}\right)^{-\frac{1}{2}}\right] \\ &= \frac{1}{2}\mathrm{erfc}\left[\left(\frac{2(1+U)}{\gamma_s}+\frac{\theta(1+U)^2}{2\gamma_s^2}\right)^{-\frac{1}{2}}\right], \quad (35)\end{aligned}$$

where $\mathrm{erfc}(x)$ is the well-known complementary error function defined as $\mathrm{erfc}(x) = \frac{2}{\sqrt{\pi}}\int_x^{\infty}e^{-t^2}\mathrm{d}t$.

C. Erroneous Code Detection Probability P_{ed}

In order to estimate the transmitted U code indices, we select U maximum absolute values of z_u, where $z_u = z_a^u + \sqrt{-1}z_b^u, u = 1, 2, \cdots, N$. The case of detecting the code indices accurately is appearing when the smallest absolute value of v^{th} (desired) decision variable is greater than the largest absolute value of w^{th} decision variable for any $w \neq v$. Otherwise, there will be an error occurring. Based on this, the erroneous code detection probability P_{ed} is given as

$$P_{ed}=1-\Pr\left\{\max_{\substack{w\in\{1,2,\cdots,N-U\}\\ w\neq v}}\{|z_w|\} < \min_{v\in\{1,2,\cdots,U\}}\{|z_v|\}\right\}. \quad (36)$$

According to the analysis of the two subsections above, since the decision variable z_a^v and z_b^v are independent of each other, the mean and variance of z_v corresponding to the correct code index detection can be calculated as

$$\begin{aligned}\mu_1 &= \mathrm{E}[z_a^v]+\mathrm{E}[z_b^v] = \sum_{l=1}^{L}\alpha_l^2\frac{(a_v+b_v)E_s}{P(1+U)} \\ &= \sqrt{\sum_{l=1}^{L}\alpha_l^2E_sN_0}\underbrace{\frac{(a_v+b_v)\sqrt{\gamma_s}}{P(1+U)}}_{\kappa}, \quad (37)\end{aligned}$$

$$\begin{aligned}\sigma_1^2 &= \mathrm{Var}[z_a^v]+\mathrm{Var}[z_b^v] \\ &= 2\left(\sum_{l=1}^{L}\alpha_l^2\frac{E_sN_0}{P^2(1+U)}+\theta\frac{N_0^2}{4P^2}\right) \\ &= \sum_{l=1}^{L}\alpha_l^2E_sN_0\underbrace{\left(\frac{2}{P^2(1+U)}+\frac{\theta}{2P^2\gamma_s}\right)}_{\lambda}. \quad (38)\end{aligned}$$

With respect to the case of $M=2$, the mean and variance of decision variable z_v are stated as

$$\begin{aligned}\mu_1 &= \sum_{l=1}^{L}\alpha_l^2\frac{E_s}{P\left(1+U\right)} \\ &= \sqrt{\sum_{l=1}^{L}\alpha_l^2 E_s N_0}\underbrace{\frac{\sqrt{\gamma_s}}{P\left(1+U\right)}}_{\kappa}, \end{aligned} \tag{39}$$

$$\begin{aligned}\sigma_1^2 &= \sum_{l=1}^{L}\alpha_l^2\frac{E_s N_0}{P^2\left(1+U\right)}+\theta\frac{N_0^2}{4P^2} \\ &= \sum_{l=1}^{L}\alpha_l^2 E_s N_0\underbrace{\left(\frac{1}{P^2\left(1+U\right)}+\frac{\theta}{4P^2\gamma_s}\right)}_{\lambda}. \end{aligned} \tag{40}$$

When the code index detection is wrong, the decision variable z_a^w can be expressed as

$$\begin{aligned}z_a^w &= \sum_{j=1}^{\theta}\left(\sum_{l=1}^{L}\alpha_l c_{x,j-\tau_l}+n_{R,j}\right)n_{I_w,j} \\ &= \sum_{j=1}^{\theta}\sum_{l=1}^{L}\alpha_l c_{x,j-\tau_l}n_{I_w,j}+\sum_{j=1}^{\theta}n_{R,j}n_{I_w,j}. \end{aligned} \tag{41}$$

Similarly, another decision variable z_b^w can be represented as

$$\begin{aligned}z_b^w &= \sum_{j=1}^{\theta}\left(\sum_{l=1}^{L}\alpha_l c_{y,j-\tau_l}+\tilde{n}_{R,j}\right)n_{I_w,j} \\ &= \sum_{j=1}^{\theta}\sum_{l=1}^{L}\alpha_l c_{y,j-\tau_l}n_{I_w,j}+\sum_{j=1}^{\theta}\tilde{n}_{R,j}n_{I_w,j}. \end{aligned} \tag{42}$$

Based on equation (41) and (42), the mean and variance of z_w will be

$$\mu_2 = \mathrm{E}\left[z_a^w\right]+\mathrm{E}\left[z_b^w\right]=0, \tag{43}$$

$$\begin{aligned}\sigma_2^2 &= \mathrm{Var}\left[z_a^w\right]+\mathrm{Var}\left[z_b^w\right] \\ &= 2\left(\sum_{l=1}^{L}\alpha_l^2\theta\mathrm{E}\left[c_j^2\right]\frac{N_0}{2P}+\theta\frac{N_0^2}{4P^2}\right) \\ &= \sum_{l=1}^{L}\alpha_l^2\frac{E_s N_0}{P^2\left(1+U\right)}+\theta\frac{N_0^2}{2P^2} \\ &= \sum_{l=1}^{L}\alpha_l^2 E_s N_0\underbrace{\left(\frac{1}{P^2\left(1+U\right)}+\frac{\theta}{2P^2\gamma_s}\right)}_{\eta}. \end{aligned} \tag{44}$$

Likewise, regarding the case of $M=2$, the mean and variance of z_w can be obtained as $\mu_2=0$ and $\sigma_2^2=\sum_{l=1}^{L}\alpha_l^2 E_s N_0\underbrace{\left(\frac{1}{2P^2\left(1+U\right)}+\frac{\theta}{4P^2\gamma_s}\right)}_{\eta}$, respectively.

It is important to note that the random variables $|z_v|$ and $|z_w|$ follow the folded normal distribution [39]. Assuming that $Y=\min\left\{|z_v|\right\}, v=1,2,\cdots,U$ and $X=\max\left\{|z_w|\right\}, w=1,2,\cdots,N-U$. Therefore, the erroneous code detection probability can be obtained as [27], [31]

$$P_{ed}=\int_0^{\infty}\left[1-F_{|z_w|}\left(y\right)\right]^{N-U}f_Y\left(y\right)\mathrm{d}y, \tag{45}$$

where $F_{|z_w|}\left(y\right)$ is the cumulative distribution function of $|z_w|$ given as

$$F_{|z_w|}\left(y\right)=\mathrm{erf}\left(\frac{y}{\sqrt{2\sigma_2^2}}\right), \tag{46}$$

where $\mathrm{erf}\left(x\right)=\frac{2}{\sqrt{\pi}}\int_0^x e^{-t^2}\mathrm{dt},\ x\geq 0$ denotes the error function. Then, $f_Y\left(y\right)$ is the probability density function of Y. Since U random variables $\left\{|z_1|,|z_2|,\cdots,|z_U|\right\}$ are independent of each other, the cumulative distribution function of Y meets

$$F_Y\left(y\right)=1-\left[1-F_{|z_v|}\left(y\right)\right]^U. \tag{47}$$

Accordingly, the probability density function of Y is the derivative of $F_Y\left(y\right)$, calculated as

$$f_Y\left(y\right)=U\left[1-F_{|z_v|}\left(y\right)\right]^{U-1}f_{|z_v|}\left(y\right), \tag{48}$$

where $f_{|z_v|}\left(y\right)$ and $F_{|z_v|}\left(y\right)$ are the probability density function and the cumulative distribution function of $|z_w|$ formulated, respectively, as

$$f_{|z_v|}\left(y\right)=\frac{1}{\sqrt{2\pi\sigma_1^2}}\left\{e^{-\frac{(y-\mu_1)^2}{2\sigma_1^2}}+e^{-\frac{(y+\mu_1)^2}{2\sigma_1^2}}\right\}, \tag{49}$$

$$F_{|z_v|}\left(y\right)=\frac{1}{2}\left[\mathrm{erf}\left(\frac{y-\mu_1}{\sqrt{2\sigma_1^2}}\right)+\mathrm{erf}\left(\frac{y+\mu_1}{\sqrt{2\sigma_1^2}}\right)\right]. \tag{50}$$

Substituting (46) and (48) into (45), and then let $y=\zeta\sqrt{\sum_{l=1}^{L}\alpha_l^2 E_s N_0}$ and $\mathrm{d}y=\sqrt{\sum_{l=1}^{L}\alpha_l^2 E_s N_0}\mathrm{d}\zeta$ into (45), thus the erroneous code detection probability P_{ed} can be rewritten as

$$\begin{aligned}P_{ed}=&\frac{1}{\sqrt{2\pi\lambda}}\int_0^{\infty}\left[1-\mathrm{erf}\left(\frac{\zeta}{\sqrt{2\eta}}\right)\right]^{N-U} \\ &\times U\left[1-F_{|z_v|}\left(\zeta\right)\right]^{U-1}\left\{e^{-\frac{(\zeta-\kappa)^2}{2\lambda}}+e^{-\frac{(\zeta+\kappa)^2}{2\lambda}}\right\}\mathrm{d}\zeta. \end{aligned} \tag{51}$$

Substituting (32) or (35) and (51) into (11), the bit error probability of CIM-OM-MDCSK system can be obtained.

In this paper, considering the case of L independent and identically distributed (i.i.d) Rayleigh-fading channels, the probability density function of the symbol-SNR γ_s can be given as [17], [37], [38]

$$f\left(\gamma_s\right)=\frac{\gamma_s^{L-1}}{(L-1)!\bar{\gamma}_c^L}\exp\left(-\frac{\gamma_s}{\bar{\gamma}_c}\right), \tag{52}$$

where $\bar{\gamma}_c=\frac{E_s}{N_0}\mathrm{E}\left[\alpha_j^2\right]=\frac{E_s}{N_0}\mathrm{E}\left[\alpha_l^2\right], j\neq l$ is the average symbol-SNR per channel and $\sum_{l=1}^{L}\mathrm{E}\left[\alpha_l^2\right]=1$. Accordingly, the averaged BER of the CIM-OM-MDCSK system over multipath Rayleigh fading channel can be calculated as

$$\bar{P}_{sys}=\int_0^{\infty}P_{sys}\cdot f(\gamma_s)\mathrm{d}\gamma_s, \tag{53}$$

where the integral in (53) is evaluated numerically.

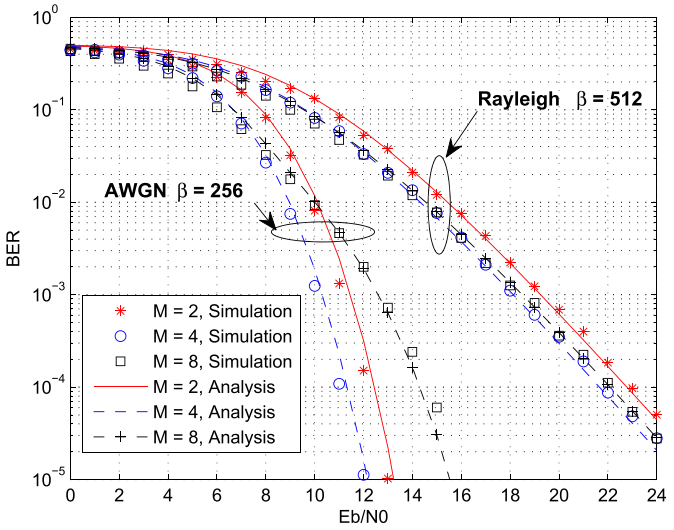

Fig. 3. BER performance of CIM-OM-MDCSK system over AWGN and multipath Rayleigh fading channel with $P = 8$, $U = 2$ and $M = 2, 4, 8$.

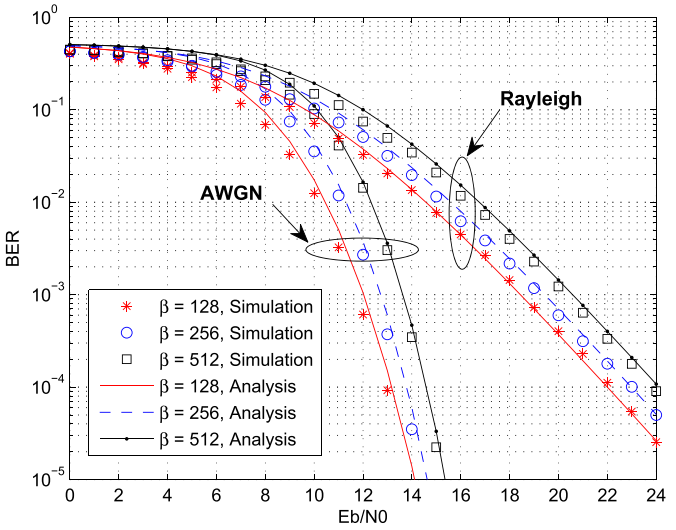

Fig. 4. BER performance of CIM-OM-MDCSK system over AWGN and multipath Rayleigh fading channel with $P = 4$, $U = 2$, $M = 4$ and $\beta = 128, 256, 512$.

IV. Numerical Results and Discussions

In this section, we evaluate the BER performance of the proposed CIM-OM-MDCSK system over AWGN and multipath Rayleigh fading channels. In this paper, the logistic map $c_{j+1} = 1 - 2c_j^2, j = 0, 1, \cdots$, is used to generate the chaotic signal. To analyse the performance in multipath Rayleigh fading channel, unless otherwise specified, a three-path channel model is considered, having the equal average power gains, i.e., $\mathrm{E}\left(\alpha_1^2\right) = \mathrm{E}\left(\alpha_2^2\right) = \mathrm{E}\left(\alpha_3^2\right) = \frac{1}{3}$, with the time delay $\tau_1 = 0, \tau_2 = T_c, \tau_3 = 2T_c$, where $T_c = 1$ is the interval of chaotic samples.

A. Performance Evaluation

To verify our theoretical derivations in the above section, the analytical results are compared with the corresponding simulation results, on the condition of both AWGN and multipath Rayleigh fading channels. As observed in Fig. 3, it is clearly discovered that the simulated results match the theoretical ones quite well over both AWGN and multipath Rayleigh fading channels. For AWGN channel, it should be noticed that the proposed CIM-OM-MDCSK system can get the best BER performance in the case of $M = 4$. However, when the modulation order is further increased, BER performance begins to deteriorate gradually. This phenomenon can be explained that when the modulation order increases, the Euclidean distance of M-ary constellation points becomes smaller, which results in the disappointing BER performance of the proposed CIM-OM-MDCSK system. As for multipth Rayleigh fading channel, the BER performance of $M = 4$ and $M = 8$ outperform the counterpart of $M = 2$.

In Fig. 4, we investigate the BER performance of CIM-OM-MDCSK sysetm over AWGN and multipath Rayleigh fading channels with $P = 4$, $U = 2$, $M = 4$ and $\beta = 128, 256, 512$. Clearly, the analytical results have a good fitting degree with the simulation results. As shown in Fig. 4, the performance gain between $\beta = 128$ and $\beta = 512$ is more than 1dB at BER level 10^{-5} in the case of AWGN channel, while the

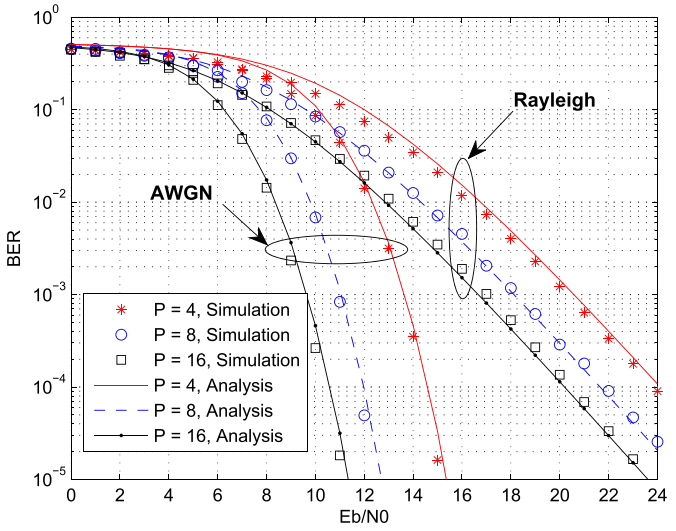

Fig. 5. The effect of P on BER performance over AWGN and multipath Rayleigh fading channels with $\beta = 512$, $U = 2$ and $M = 4$.

performance improvement of $\beta = 128$ over $\beta = 512$ is 2dB at BER level 10^{-4} in the case of multipath Rayleigh fading channel. It indicates that the BER performance of the proposed CIM-OM-MDCSK system degrades with the increasing of spreading factor. To explain this phenomenon, we can elaborate that the contribution of noise-noise cross correlation term becomes more significant for high spreading factor, which causes the degradation of CIM-OM-MDCSK BER performance.

In order to further make clear the behavior of the CIM-OM-MDCSK system, the influence of different orders of Walsh code on the BER Performance is discussed. As shown in Fig. 5, it is clearly found that, on the condition of the identical spreading factor, the BER performance of CIM-OM-MDCSK system over AWGN channel keeps an ameliorative trend as the order of Walsh code arguments. This is owing to the fact that more bits will be mapped within a

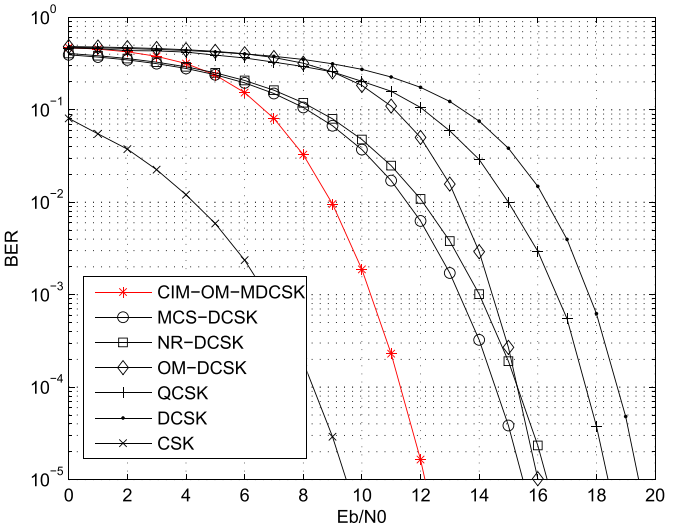

Fig. 6. BER performance comparisons of CIM-OM-MDCSK to other up-to-date chaotic communication systems over AWGN channel with $\beta = 256$.

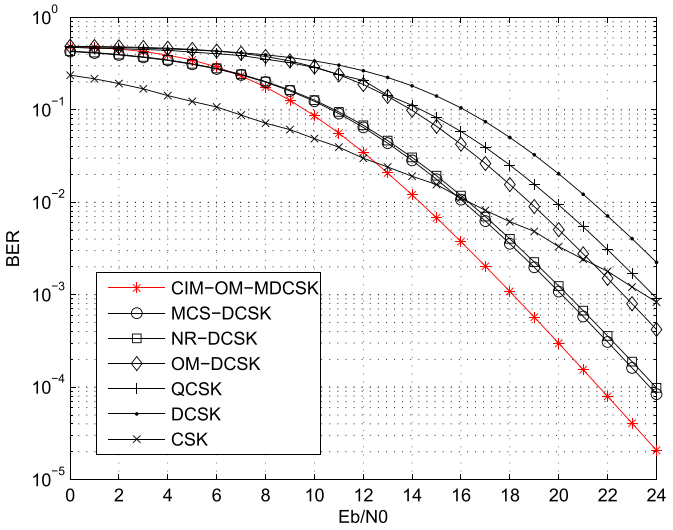

Fig. 7. BER performance comparisons of CIM-OM-MDCSK to other up-to-date chaotic communication systems over multipath Rayleigh fading channel with $\beta = 512$.

symbol for the same transmitted energy when P increases. As a result, the required SNR needed to achieve a given BER level reduces. For example, the CIM-OM-MDCSK system will need slightly greater than 15dB to achieve 10^{-5} BER level when $P = 4$. By contrast, in the case of $P = 16$, the required SNR is about 11dB at the same BER level above. In other words, the performance gain is approximate 4dB between $P = 16$ and $P = 4$. From another perspective, there is a perfect match between the simulation results and the corresponding theoretical results. As illustrated in Fig. 5, regarding to multipath Rayleigh fading channel, the proposed CIM-OM-MDCSK system wins preferable BER performance when P increases, which is similar to the case of AWGN channel. In particular, the BER performance gap of CIM-OM-MDCSK system between $P = 16$ and $P = 4$ is close to 4dB at BER level 10^{-4}. Predictably, the BER performance improvement will become more remarkable as P enlarges.

In order to verify the outstanding performance of the proposed CIM-OM-MDCSK system, we make a comparison between the proposed system and other up-to-date non-coherent chaotic communication systems over AWGN and multipath Rayleigh fading channels, and the coherent CSK system is listed as well for reference. Except for special statements, the order of the Walsh code is equal to $P = 8$ for all systems. Firstly, we consider MCS-DCSK, OM-DCSK, NR-DCSK, QCSK and DCSK as comparison objects of CIM-OM-MDCSK system. In NR-DCSK system, the window size of moving average filter is set to 16. Then, $U = 2$ and $M = 4$ are provided for the simulation of CIM-OM-MDCSK system. In the case of AWGN channel, as displayed in Fig. 6, the best BER performance within the comparison systems is MCS-DCSK system, which can achieve more than 4dB performance improvement compared to the worst DCSK system at the BER of 10^{-5}. However, it should be notice that the BER performance gain between CIM-OM-MDCSK and DCSK system has reached 7dB at the same BER level above, which means the proposed CIM-OM-MDCSK system is highly immune to noise jamming. As for the case of multipath Rayleigh fading channel, the performance contrasts of the proposed CIM-OM-MDCSK system and other chaotic communication systems are depicted in Fig. 7. In particular, the performance improvement for recently designed NR-DCSK system over QCSK system is about 4dB at a BER of 10^{-3}. As a contrast, the proposed CIM-OM-MDCSK system performs 6dB better than QCSK system at BER level 10^{-3}. Although the coherent CSK system can obtain more than 2dB BER performance improvement with comparison to the proposed CIM-OM-MDCSK system at the BER level 10^{-5} in AWGN channel, on the contrary, the CIM-OM-MDCSK system can receive about 6dB BER performance gain compared to CSK system at a BER 10^{-3} in multipath Rayleigh fading channel. On the other hand, since the locally-generated carriers have to be synchronized at the CSK receiver, the application of CSK system is more complicated than CIM-OM-MDCSK system.

Additionally, to further highlight the superiority of the CIM-OM-MDCSK system, the BER performance comparison of CIM-OM-MDCSK system is extended to other state-of-the-art chaotic communication systems with index modulation or code index modulation, including CIM-DCSK, CIM-CS-DCSK, CCI-DCSK and PI-DCSK, over AWGN and multipath Rayleigh fading channels. For the convenience of the reader's understanding, the simulation parameters are provided for different systems as follows. In the proposed CIM-OM-MDCSK system, the parameters are set as $P = 8$, $U = 1$ and $M = 4$. Respecting CIM-CS-DCSK system, $Q_c = 1$ is provided for its simulation where Q_c denotes the total number of the transmitted bit streams and $P = 8$. As for CCI-DCSK system, the number of commutated orthogonal version of the reference signal is equal to 8. With respect to PI-DCSK system, the main parameter is the specific modulation order M_t which is set to 16.

As clearly observed in Fig. 8, the CIM-OM-MDCSK system outperforms other state-of-the-art non-coherent chaotic

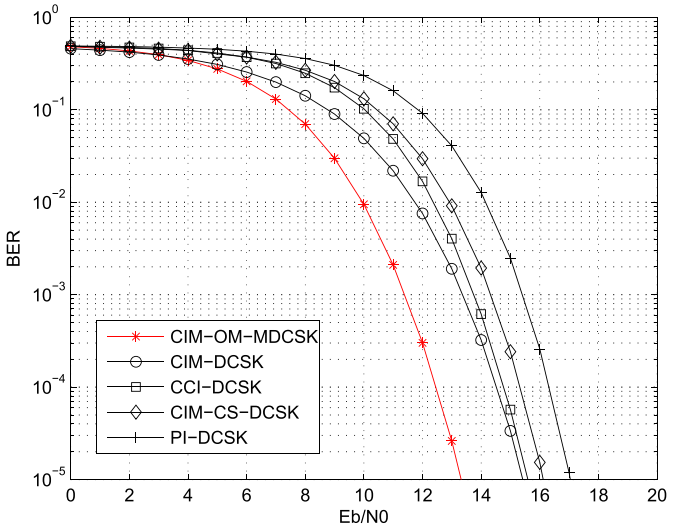

Fig. 8. BER performance comparisons of CIM-OM-MDCSK to other state-of-the-art non-coherent chaotic communication systems with index modulation or code index modulation over AWGN channel with $\beta = 256$.

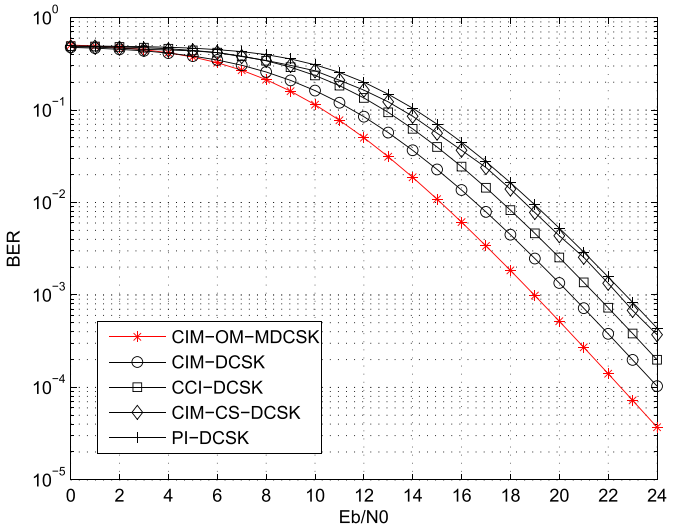

Fig. 9. BER performance comparisons of CIM-OM-MDCSK to other state-of-the-art non-coherent chaotic communication systems with index modulation or code index modulation over multipath Rayleigh fading channel with $\beta = 512$.

communication systems with index modulation or code index modulation over AWGN channel. For example, the performance improvement for the proposed CIM-OM-MDCSK system over CIM-DCSK is greater than 2dB at BER level 10^{-5}, while the performance gain of CIM-OM-MDCSK system over the counterpart of PI-DCSK system is more than 4dB at the same BER level above. Likewise, among all comparison systems, the proposed CIM-OM-MDCSK system shows the best BER performance over multipath Rayleigh fading channel as shown in Fig. 9. To be specific, the performance improvement for CIM-OM-MDCSK system over other chaotic communication systems with index modulation or code index modulation is $1.5 \sim 4$dB at BER level 10^{-3}.

In Fig. 10, the BER performance of CIM-OM-MDCSK system is compared with the counterparts of other up-to-date IM-based chaotic communication systems over two-path

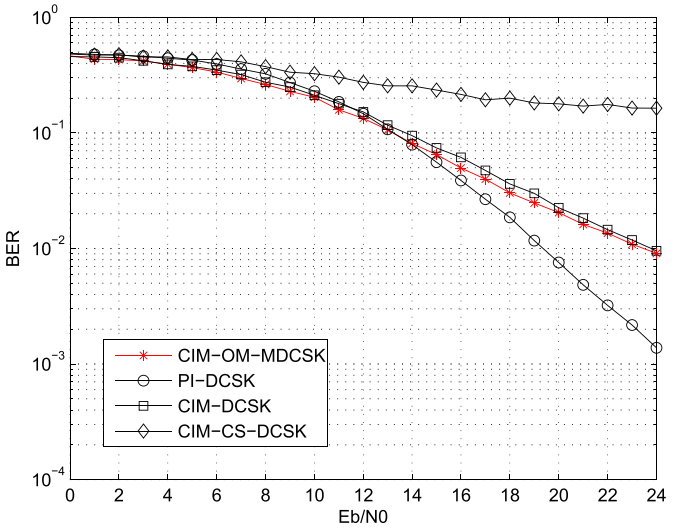

Fig. 10. BER performance comparisons between CIM-OM-MDCSK system and other up-to-date IM-based chaotic communication systems over two-path Rayleigh fading channel with $\tau_{\max} = 20$ and $\beta = 128$.

Rayleigh fading channel with significant inter symbol interference. Explicitly, the channel parameters are set to the equal average power gain $\mathrm{E}\left(\alpha_1^2\right) = \mathrm{E}\left(\alpha_2^2\right) = \frac{1}{2}$ and the maximum channel delay $\tau_{\max} = 20$. In CIM-OM-MDCSK system, the parameters $P = 4$, $U = 1$ and $M = 4$ are used for its simulation. The specific modulation order M_t is equal to 8 in PI-DCSK system, while the order of Walsh code $P = 4$ is adopted for CIM-DCSK system. Then $P = 8$ and $Q_c = 1$ are applied for the simulation of CIM-CS-DCSK system. As observed from the simulation parameters, we can make a conclusion that the overall number of transmitted bits per symbol is equal to 3 for all systems above. Although the CIM-OM-MDCSK system can still win the better BER performance compared to CIM-DCSK and CIM-CS-DCSK systems, the BER performance of CIM-OM-MDCSK system is distinctly second place in contrast to PI-DCSK system. This phenomenon is attributed to the fact that the cross correlation of different Walsh code sequences significantly reduces when the Walsh code sequences are not perfectly matched, namely, the effect of inter symbol interference is very large.

As clearly witnessed in all the figures above, a significant conclusion surfaces in front of us. The proposed CIM-OM-MDCSK system performs well in the environment of noise jamming and shows higher resistance for the fading propagation environment compared to other non-coherent chaotic communication systems, which is especially suitable for the rugged environment of future wireless communication.

V. Conclusions

In this paper, we have proposed an M-ary orthogonal multilevel differential chaos shift keying system with code index modulation. Since the reference signal and information bearing signals are overlapping within the same time slot, the spectral efficiency of the proposed system can be significantly improved. Moreover, due to the benefits of code index modulation, which comes up with new dimensions for conveying digital information, the spectral efficiency of the considered system is further increased.

From another perspective, by combining the M-ary modulation, multilevel modulation and code index modulation, the CIM-OM-MDCSK system achieves high data rate and excellent BER performance. In addition, the implement of Hilbert filter, k-combinations mapper and several delay units make CIM-OM-MDCSK system more complicated in contrast to PI-DCSK and CIM-DCSK systems. However, it is by means of the price of hardware complexity that the proposed CIM-OM-MDCSK system harvests the improvement of the data rate and BER performance to a great extent. The BER performance comparisons between the proposed CIM-OM-MDCSK system and other state-of-the-art chaotic communication systems verified the excellent performance of the proposed system. In conclusion, the proposed CIM-OM-MDCSK system is a competitive and promising system that can meet the demands of high data rate, and offer excellent BER performance even in severe fading channel environment.

REFERENCES

[1] F. C. M. Lau and C. K. Tse, *Chaos-Based Digital Communication Systems*. New York, NY, USA: Springer, 2003.

[2] L. Ye, G. Chen, and L. Wang, "Essence and advantages of FM-DCSK versus conventional spread-spectrum communication methods," *Circuits, Syst. Signal Process.*, vol. 24, no. 5, pp. 657–673, Sep. 2005.

[3] Y. Fang, G. Han, P. Chen, F. C. M. Lau, G. Chen, and L. Wang, "A survey on DCSK-based communication systems and their application to UWB scenarios," *IEEE Commun. Surveys Tuts.*, vol. 18, no. 3, pp. 1804–1837, 3rd Quart., 2016.

[4] X. Min, W. Xu, L. Wang, and G. Chen, "Promising performance of a frequency-modulated differential chaos shift keying ultra-wideband system under indoor environments," *IET Commun.*, vol. 4, no. 2, pp. 125–134, Jan. 2010.

[5] G. Kolumbán, "UWB technology: Chaotic communications versus noncoherent impulse radio," in *Proc. ECCTD*, Cork, Ireland, Sep. 2002, pp. 79–82.

[6] S. Chen, L. Wang, and G. Chen, "Data-aided timing synchronization for FM-DCSK UWB communication systems," *IEEE Trans. Ind. Electron.*, vol. 57, no. 5, pp. 1538–1545, May 2010.

[7] U. Parlitz, L. O. Chua, L. Kocarev, K. S. Halle, and A. Shang, "Transmission of digital signals by chaotic synchronization," *Int. J. Bifurcation Chaos*, vol. 2, no. 4, pp. 973–977, 1992.

[8] G. Kolumbán, G. K. Vizvári, W. Schwarz, and A. Abel, "Differential chaos shift keying: A robust coding for chaos communication," in *Proc. Nonlinear Dyn. Electron. Syst.*, Seville, Spain, 1996, pp. 92–97.

[9] M. P. Kennedy, G. Kolumbán, G. Kis, and Z. Jako, "Performance evaluation of FM-DCSK modulation in multipath environments," *IEEE Trans. Circuits Syst. I, Reg. Papers*, vol. 47, no. 12, pp. 1702–1711, Dec. 2000.

[10] C.-C. Chong and S. K. Yong, "UWB direct chaotic communication technology for low-rate WPAN applications," *IEEE Trans. Veh. Technol.*, vol. 57, no. 3, pp. 1527–1536, Mar. 2008.

[11] Y. Fang, L. Xu, L. Wang, and G. Chen, "Performance of MIMO relay DCSK-CD systems over Nakagami fading channels," *IEEE Trans. Circuits Syst. I, Reg. Papers*, vol. 60, no. 3, pp. 757–767, Mar. 2013.

[12] W. Xu, L. Wang, and G. Chen, "Performance of DCSK cooperative communication systems over multipath fading channels," *IEEE Trans. Circuits Syst. I, Reg. Papers*, vol. 58, no. 1, pp. 196–204, Jan. 2011.

[13] G. Kaddoum and N. Tadayon, "Differential chaos shift keying: A robust modulation scheme for power-line communications," *IEEE Trans. Circuits Syst., II, Exp. Briefs*, vol. 64, no. 1, pp. 31–35, Jan. 2017.

[14] F. J. Escribano, G. Kaddoum, A. Wagemakers, and P. Giard, "Design of a new differential chaos-shift-keying system for continuous mobility," *IEEE Trans. Commun.*, vol. 64, no. 5, pp. 2066–2078, May 2016.

[15] G. Kaddoum, H.-V. Tran, L. Kong, and M. Atallah, "Design of simultaneous wireless information and power transfer scheme for short reference DCSK communication systems," *IEEE Trans. Commun.*, vol. 65, no. 1, pp. 431–443, Jan. 2017.

[16] Z. Galias and G. M. Maggio, "Quadrature chaos-shift keying: Theory and performance analysis," *IEEE Trans. Circuits Syst. I, Fundam. Theory Appl.*, vol. 48, no. 12, pp. 1510–1519, Dec. 2001.

[17] L. Wang, G. Cai, and G. R. Chen, "Design and performance analysis of a new multiresolution M-ary differential chaos shift keying communication system," *IEEE Trans. Wireless Commun.*, vol. 14, no. 9, pp. 5197–5208, Sep. 2015.

[18] S. Wang and X. Wang, "M-DCSK-Based chaotic communications in MIMO multipath channels with no channel state information," *IEEE Trans. Circuits Syst., II, Exp. Briefs*, vol. 57, no. 12, pp. 1001–1005, Dec. 2010.

[19] G. Kis, "Performance analysis of chaotic communication systems," Ph.D. dissertation, Dept. Meas. Inf. Syst., Budapest Univ. Technol. Econ., Budapest, Hungary, 2005.

[20] W. Xu, L. Wang, and G. Kolumbán, "A novel differential chaos shift keying modulation scheme," *Int. J. Bifurcation Chaos*, vol. 21, no. 3, pp. 799–814, 2011.

[21] W. Xu, L. Wang, and G. Kolumbán, "A new data rate adaption communications scheme for code-shifted differential chaos shift keying modulation," *Int. J. Bifurcation Chaos*, vol. 22, no. 8, pp. 1–8, 2012.

[22] G. Kaddoum and F. Gagnon, "Design of a high-data-rate differential chaos-shift keying system," *IEEE Trans. Circuits Syst. II, Exp, Briefs*, vol. 59, no. 7, pp. 448–452, Jul. 2012.

[23] T. Huang, L. Wang, W. Xu, and F. C. M. Lau, "Multilevel code-shifted differential-chaos-shift-keying system," *IET Commun.*, vol. 10, no. 10, pp. 1189–1195, Jul. 2016.

[24] H. Yang, W. K. S. Tang, G. Chen, and G.-P. Jiang, "System design and performance analysis of orthogonal multi-level differential chaos shift keying modulation scheme," *IEEE Trans. Circuits Syst. I, Reg. Papers*, vol. 63, no. 1, pp. 146–156, Jan. 2016.

[25] E. Basar, M. Wen, R. Mesleh, M. Di Renzo, Y. Xiao, and H. Haas, "Index modulation techniques for next-generation wireless networks," *IEEE Access*, vol. 5, pp. 16693–16746, 2017.

[26] M. Herceg, D. Vranješ, G. Kaddoum, and E. Soujeri, "Commutation code index DCSK modulation technique for high-data-rate communication systems," *IEEE Trans. Circuits Syst., II, Exp. Briefs*, vol. 65, no. 12, pp. 1954–1958, Dec. 2018.

[27] M. Herceg, G. Kaddoum, D. Vranješ, and E. Soujeri, "Permutation index DCSK modulation technique for secure multiuser high-data-rate communication systems," *IEEE Trans. Veh. Technol.*, vol. 67, no. 4, pp. 2997–3011, Apr. 2018.

[28] G. Kaddoum, M. F. A. Ahmed, and Y. Nijsure, "Code index modulation: A high data rate and energy efficient communication system," *IEEE Commun. Lett.*, vol. 19, no. 2, pp. 175–178, Feb. 2015.

[29] G. Kaddoum, Y. Nijsure, and T. Hung, "Generalized code index modulation technique for high-data-rate communication systems," *IEEE Trans. Veh. Technol.*, vol. 65, no. 9, pp. 7000–7009, Sep. 2016.

[30] G. Kaddoum and E. Soujeri, "On the comparison between code-index modulation and spatial modulation techniques," in *Proc. Int. Conf. Inf. Commun. Technol. Res. (ICTRC)*, Abu Dhabi, UAE, May 2015, pp. 24–27.

[31] W. Xu, T. Huang, and L. Wang, "Code-shifted differential chaos shift keying with code index modulation for high data rate transmission," *IEEE Trans. Commun.*, vol. 65, no. 10, pp. 4285–4294, Oct. 2017.

[32] G. Kaddoum, E. Soujeri, and Y. Nijsure, "Design of a short reference noncoherent chaos-based communication systems," *IEEE Trans. Commun.*, vol. 64, no. 2, pp. 680–689, Jan. 2016.

[33] W. Xu, Y. Tan, F. C. M. Lau, and G. Kolumbán, "Design and optimization of differential chaos shift keying scheme with code index modulation," *IEEE Trans. Commun.*, vol. 66, no. 5, pp. 1970–1980, May 2018.

[34] G. Kaddoum and E. Soujeri, "NR-DCSK: A noise reduction differential chaos shift keying system," *IEEE Trans. Circuits Syst., II, Exp. Briefs*, vol. 63, no. 7, pp. 648–652, Jul. 2016.

[35] W. Xu and L. Wang, "Performance optimization for short reference differential chaos shift keying scheme," in *Proc. IEEE Int. Conf. Signal Process., Commun. Comput. (ICSPCC)*, Xiamen, China, Oct. 2017, pp. 1–6.

[36] Y. Xia, C. K. Tse, and F. C. M. Lau, "Performance of differential chaos-shift-keying digital communication systems over a multipath fading channel with delay spread," *IEEE Trans. Circuits Syst., II, Exp. Briefs*, vol. 51, no. 12, pp. 680–684, Dec. 2004.

[37] G. Kaddoum, F.-D. Richardson, and F. Gagnon, "Design and analysis of a multi-carrier differential chaos shift keying communication system," *IEEE Trans. Commun.*, vol. 61, no. 8, pp. 3281–3291, Aug. 2013.

[38] J. G. Proakis and M. Salehi, *Digital Communications*. New York, NY, USA: McGraw-Hill, 2007.

[39] A. Papoulis and S. Pillai, *Probability–Random Variables and Stochastic Processes*. New York, NY, USA: McGraw-Hill, 1991.

Xiangming Cai received the B.Sc. degree in information engineering from the Guangdong University of Technology, Guangzhou, China, in 2017. He is currently pursuing the M.Sc. degree with the Department of Information and Communication Engineering, Xiamen University, Fujian, China. His research interests include chaos-based digital communications and their applications to wireless communications.

Weikai Xu (S'10–M'12) received the B.S. degree in electronic engineering from Chongqing Three Gorges College, Chongqing, China, in 2000, the M.Sc. degree in communication and information system from the Chongqing University of Posts and Telecommunications, Chongqing, in 2003, and the Ph.D. degree in electronic circuit and system from the Xiamen University, Xiamen, China, in 2011. From 2003 to 2012, he was a Teaching Assistant and an Assistant Professor in communication engineering with Xiamen University, where he is currently an Associate Professor in information and communication engineering. His research interests include chaotic communications, underwater acoustic communications, channel coding, cooperative communications, and ultra-wideband.

Deqing Wang received the Ph.D. degree in communication engineering from Xiamen University, Xiamen, China, in 2013. He was with the Georgia Institute of Technology as a Visiting Scholar from 2016 to 2017. He is currently an Assistant Professor with the Key Laboratory of Underwater Acoustic Communication and Marine Information Technology, Xiamen University, Ministry of Education. His research interests include underwater acoustic communication and networking, underwater acoustic signal processing, and underwater acoustic physical-layer network coding.

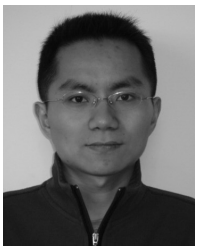

Shaohua Hong (M'12) received the B.Sc. degree in electronics and information engineering from Zhejiang University, Hangzhou, China, in 2005, and the Ph.D. degree in electronics science and technology from Zhejiang University, Hangzhou, China, in 2010. He is currently an Associate Professor with the Department of Information and Communication Engineering, Xiamen University, Xiamen, China. His research interests include joint source and channel coding, wireless communication, and image processing. He has been serving as an Editor for *KSII Transactions on Internet and Information Systems* since 2015.

Lin Wang (S'99–M'03–SM'09) received the M.Sc. degree in applied mathematics from the Kunming University of Technology, China, in 1988, and the Ph.D. degree in electronics engineering from the University of Electronic Science and Technology of China, China, in 2001. From 1984 to 1986, he was a Teaching Assistant with the Mathematics Department, Chongqing Normal University. From 1989 to 2002, he was a Teaching Assistant, a Lecturer, and an Associate Professor in applied mathematics and communication engineering with the Chongqing University of Posts and Telecommunications, China. From 1995 to 1996, he was with the Mathematics Department, University of New England, Armidale, NSW, Australia. In 2003, he was a Visiting Researcher with the Center for Chaos and Complexity Networks, Department of Electronic Engineering, City University of Hong Kong, for three months. In 2013, he was a Senior Visiting Researcher with the Department of ECE, University of California at Davis, Davis, CA, USA. From 2003 to 2012, he was a Full Professor and an Associate Dean with the School of Information Science and Engineering, Xiamen University, China, where he has been a Distinguished Professor since 2012. He has authored more than 100 journals and conference papers. He holds 14 patents in the field of physical layer in digital communications. His current research interests are in the areas of channel coding, joint source and channel coding, chaos modulation, and their applications to wireless communication and storage systems.